Supporting Information

Zhu et al. 10.1073/pnas.1800182115

SI Materials and Methods

For live cell imaging, seedlings were grown vertically on MS plates in dark for 2.5 d. Images were taken from the epidermal cells about 2 mm below the apical hook. Imaging was performed on a Yokogawa CSUX1 spinning-disk system featuring a DMI6000 Leica motorized microscope, a Photometrics QuantEM: 512SC CCD camera, and a Leica 100 × 1.4 numerical aperture oil objective. An ATOF laser with three laser lines (440/491/561 nm) was used to enable fast switching between different excitations. Band-pass filters (520/50 nm for GFP, 620/60 nm for RFP) were used for emission filtering. Image analysis was performed using Metamorph (Molecular Devices), Imaris (Bitplane) and Fiji (ImageJ) (v2.0.0-rc-43/1.51 h).

For the particle lifetime analysis, 60-s time-series movies with 1-s intervals were obtained. The particles' lifetime on the PM was measured according to the kymographs derived from the movies.

For the colocalization analyses, single-frame images from both channels (520/50 nm for YFP and 620/60 nm for RFP) were taken simultaneously. The colocalized particles were manually selected in Fiji and percentage of colocalization was calculated.

For CESA particle dynamics analyses, 5-min time-series movies with 5-s intervals were obtained from several cells in each genotypes. Velocities of CESA particles were measured automatically using Imaris.

For the FRAP assay, an 8-min movie with 5-s interval was obtained (in the case of RFP–PTL1 YFP–CESA6, the interval was set to 1 s). Upon 20 s after filming, an area of 200 × 80 pixel^2 was photobleached using the iLAS^2 system (Roper Scientific). Newly delivered particles were manually selected at desired time following photobleaching.

For CESA particle density analyses, a single optical section image was taken at the PM focal plane. In ImageJ, an ROI avoiding Golgi signal-masked area was selected using the "Freehand selections" tool. The area of ROI was determined by the "Measure" function, and the CESA particles within the ROI were detected using the "find maxima" tool.

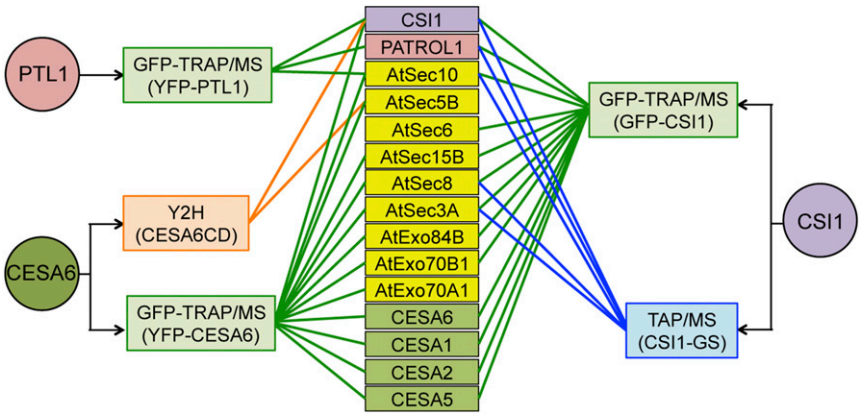

Fig. S1. Overview of interactions among the exocyst complex, CSI1, PTL1, and CSCs. An interactive network summarizing all of the interactions detected from the current work. Round shapes represent all of the protein baits. Red, PATROL1; green, CESA6; purple, CSI1. Different experimental methods are described in the boxes next to the baits. Proteins identified from all of the experiments are listed in the middle with different colors. Purple, CSI1; red, PATROL1; yellow, subunits of the exocyst complex; green, subunits of CSCs. Connecting lines correspond to positive interactions between prey protein and bait protein.

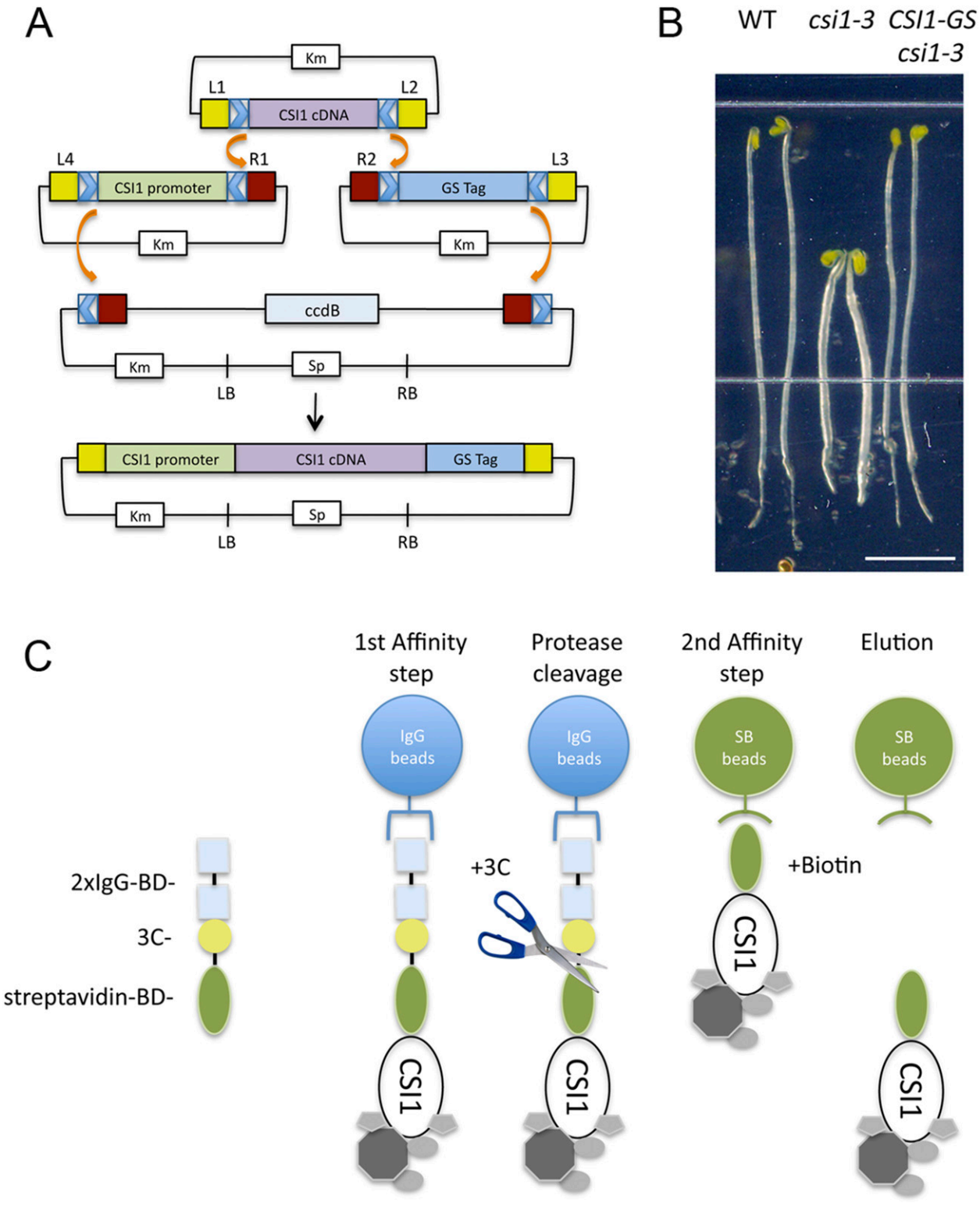

Fig. S2. Biochemical purification of the CSI1-associated protein complex. (*A*) A schematic representation of the GS-tagged CSI1 construct (CSI1–GS). (*B*) Images of 4-d-old etiolated *Arabidopsis* seedlings showing that CSI1-GS fully complement *csi1-3* mutant defects. (Scale bar, 0.5 cm.) (*C*) Schematic representation of affinity purification of CSI1-associated protein complex. Purification procedure consists of four steps: (*i*) Protein extracts are incubated with IgG beads. (*ii*) Elution of tagged proteins involves specific cleavage on the tag by low temperature active rhinovirus 3 C protease (3C). (*iii*) IgG bead eluates are incubated with streptavidin beads (SB). (*iv*) Elution of proteins from beads using biotin.

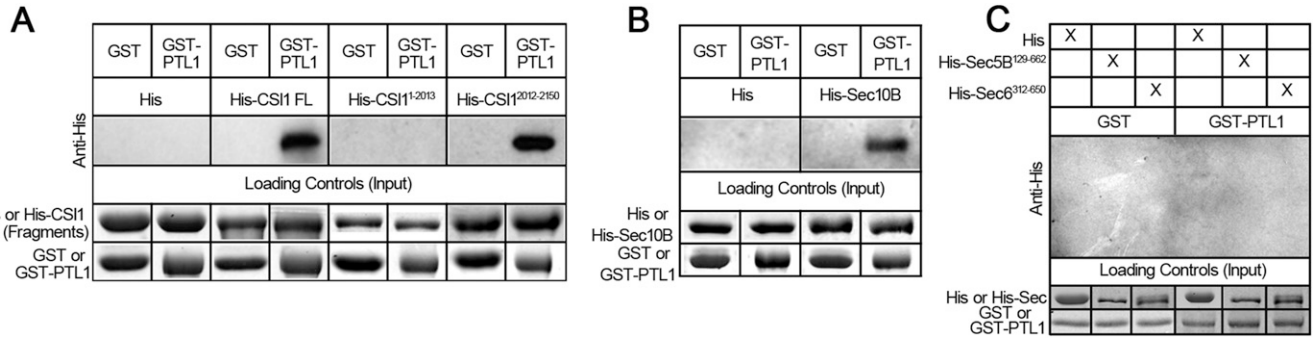

Fig. S3. In vitro interaction among CSI1, PTL1, and exocyst subunits. (*A*) CSI1 interacts with PTL1 through its C2 domain. In vitro pull-down assays show that both the His-tagged CSI1 full-length protein and the C2 domain of CSI1 ($CSI1^{2,012–2,150}$) were pulled down by GST-PTL1. Empty GST beads and the His-empty vector were used as negative controls. (*B*) PTL1 interacts with Sec10B in vitro. His-Sec10 coprecipitated with GST-PTL1 in the in vitro pull-down assay. Empty GST beads and the His-empty vector were used as negative controls. (*C*) No interaction was detected between GST-tagged PATROL1 (GST–PTL1) and His-tagged truncation of Sec5B (His-$Sec5B^{129–662}$), or GST–PTL1 and His-tagged truncation of Sec6 (His-$Sec6^{312–650}$) Empty GST beads and the His-empty vector were used as negative controls.

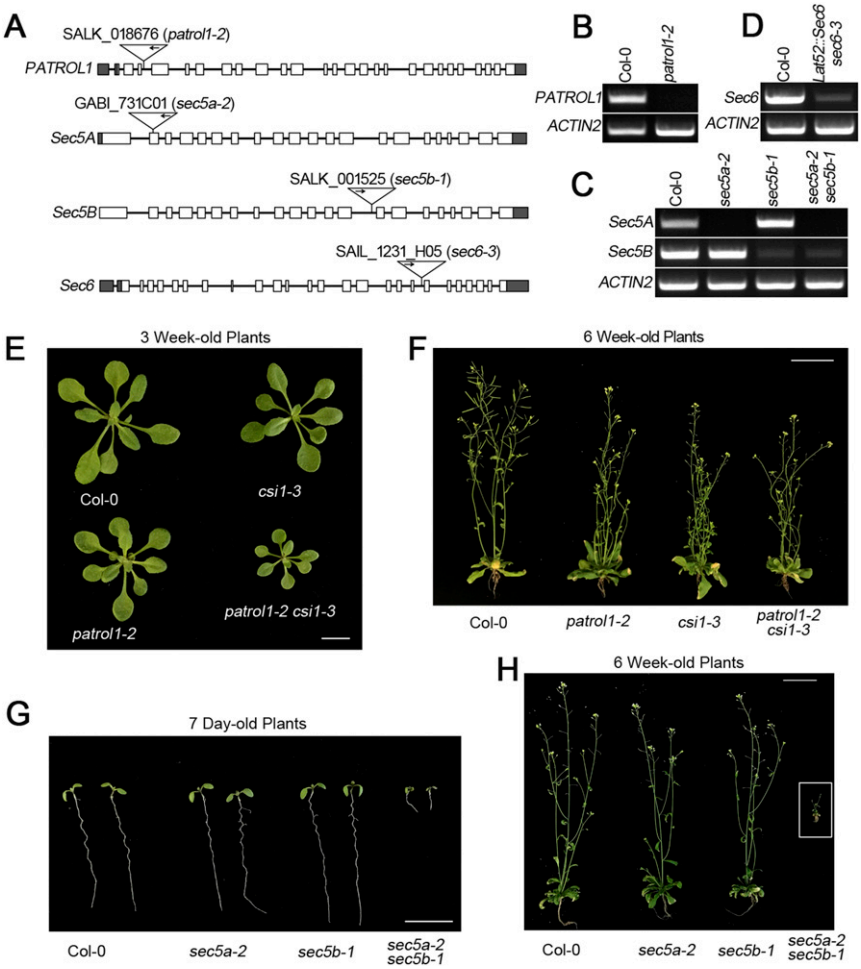

Fig. S4. T-DNA mutants used in this study and their corresponding phenotypes. (*A*) Gene structures of *PATROL1*, *Sec5A*, *Sec5B*, and *Sec6* and their corresponding T-DNA mutants used in the present study. White boxes represent exons; gray boxes represent untranslated regions (UTRs). Triangles indicate the positions of T-DNA insertions. (*B–D*) RT-PCR analysis of RNA from *sec5a-2*, *sec5b-1*, *sec5a-2 sec5b-1*, *patrol1-2*, and *pLat52::Sec6 sec6-3*. ACTIN2 was used as the reference gene. (*E* and *F*) Images of 3-wk-old plants (*E*) and 6-wk-old adult plants (*F*) of the WT (Col-0), *patrol1-2*, *csi1-3*, and *patrol1-2 csi1-3* mutants. (Scale bars, 1 cm.) (*G* and *H*) Images of 7-d-old seedlings (*G*) and 6-wk-old adult plants (*H*) of the WT (Col-0), *sec5a-2*, *sec5b-1*, and *sec5a-2 sec5b-1* (boxed) mutants. (Scale bar, 1 cm.)

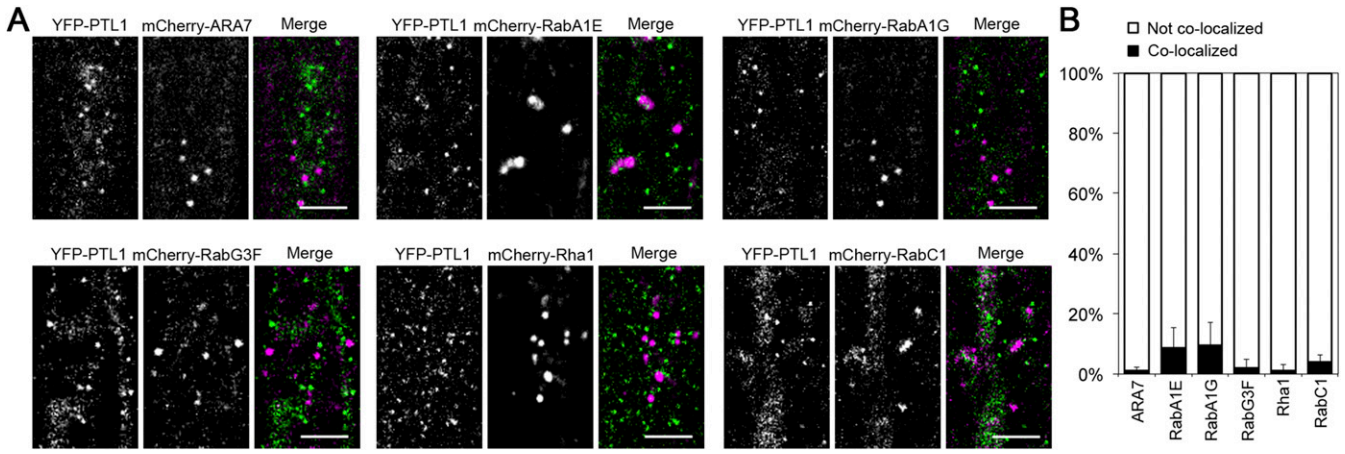

Fig. S5. PTL1 particles do not colocalize with the endosomal markers. (*A*) Single-frame images were obtained from the YFP–PTL1 and mCherry-endosomal markers simultaneously; and merged into one frame to visualize colocalized particles. (Scale bars, 5 μm.) (*B*) Quantifications of colocalization of YFP–PTL1 particles with the various endosomal markers displayed in *A*. n = 195 particles from six cells for mCherry-ARA7, n = 363 particles from nine cells for mCherry-RabA1E, n = 187 particles from eight cells for mCherry-RabA1G, n = 288 particles from seven cells for mCherry-RabG3F, n = 250 particles from six cells for mCherry-Rha1, n = 96 particles from five cells for mCherry-RabC1. Error bars represent SD.

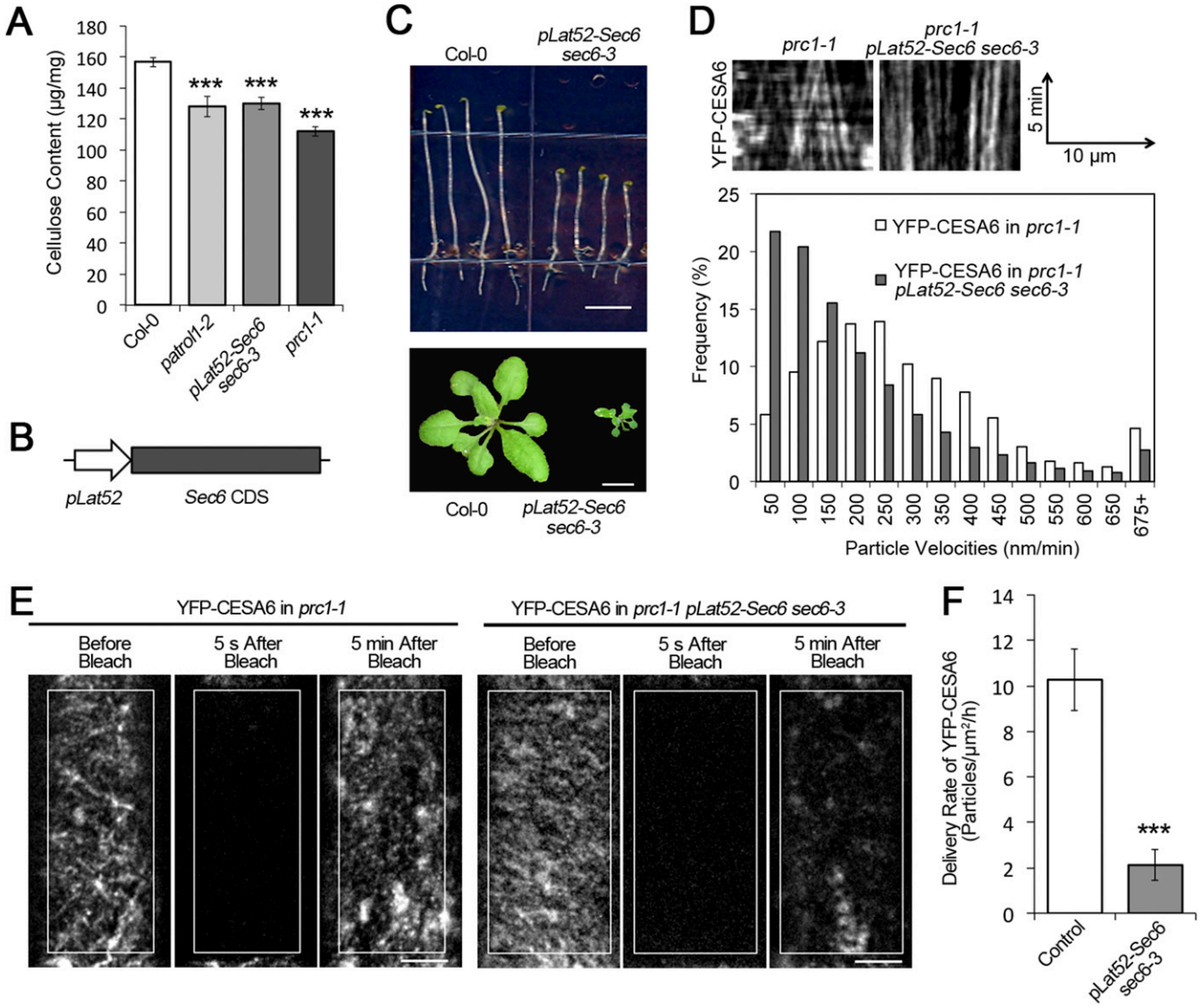

Fig. S6. Mutation of *Sec6* lead to defects in growth, cellulose production, CSCs delivery, as well as PM CSCs motilities. (*A*) Crystalline cellulose content is reduced in both *patrol1-2* and mutants of exocyst subunits. The *CESA6* mutant *prc1-1* is used as an experimental control. Error bars represent SD. ***$P < 0.0001$ ($n = 6$ replicates per genotype). (*B*) A schematic representation of *pLat52::Sec6* construct in which the expression of the *Sec6* gene is driven by the pollen-specific *Lat52* promoter. (*C*) The *pLat52::Sec6 sec6-3* transgenic lines display dwarf phenotypes. Images were taken from 4-d-old etiolated seedlings (*Upper*) and 4-wk-old rosette leaves (*Lower*). [Scale bars, 0.5 cm (*Upper*) and 1 cm (*Lower*).] (*D*) Mutation of *Sec6* results in reduced motility of PM CSCs. Kymographs were derived from 5-min movies with 5-s intervals (*Upper*). Histograms display the distribution of CSC particle velocities calculated from the kymographs (*Lower*). Average velocity in control line is 295.90 ± 200.38 nm/min; average velocity in the *Sec6* mutant line is 202.27 ± 187.90 nm/min. $n = 5137$ particles from six cells in the control line (YFP–CESA6 in *prc1-1*), $n = 6{,}583$ particles from seven cells in the *Sec6* mutant line (YFP–CESA6 in *prc1-1 pLat52::Sec6 sec6-3*). (*E*) Single-frame images displaying the PM CSCs before, 5 s and 5 min after photobleaching. FRAP assays were performed in the control YFP–CESA6 in *prc1-1* lines and the *pLat52::Sec6 sec6-3* transgenic lines. White boxes mark the photobleached area. (Scale bars, 5 μm.) (*F*) Quantifications of the delivery rate of CSCs from the FRAP assays descripted in *E*. $n = 24$ ROIs from 10 cells for the YFP–CESA6 control line; $n = 15$ ROIs from eight cells for the *Sec6* mutant line (YFP–CESA6 in *pLat52::Sec6 sec6-3 prc1-1*); Error bars represent SD. ***$P < 0.0001$.

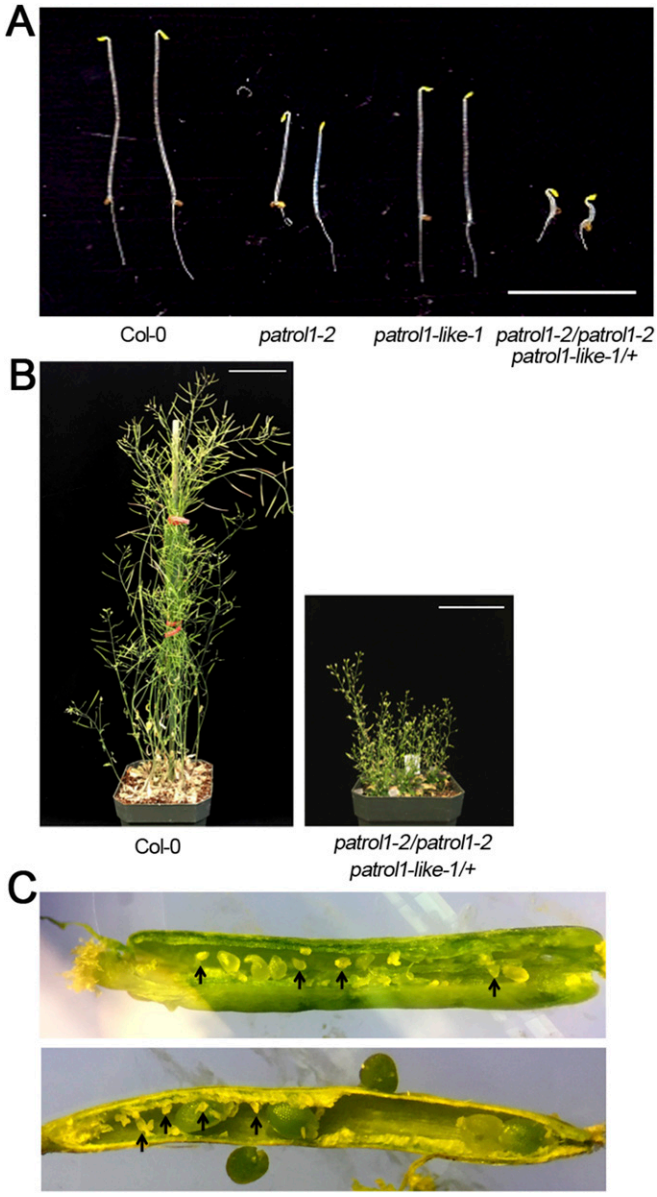

Fig. S7. *PATROL1* and *PATROL1-LIKE* genes have redundant functions. (*A*) The 3-d-old etiolated seedlings of WT (Col-0), *patrol1-2* homozygous, *patrol1-like-1* homozygous, and *patrol1-2/patrol1-2 patrol1-like-1*/+ plants. (Scale bar, 1 cm.) (*B*) Images of 7-wk-old plants of the WT (Col-0) and *patrol1-2/patrol1-2 patrol1-like-1*/+. (Scale bar, 5 cm.) (*C*) Opened siliques from the *patrol1-2/patrol1-2 patrol1-like-1*/+ plants. Arrows point to embryo-lethal seeds.

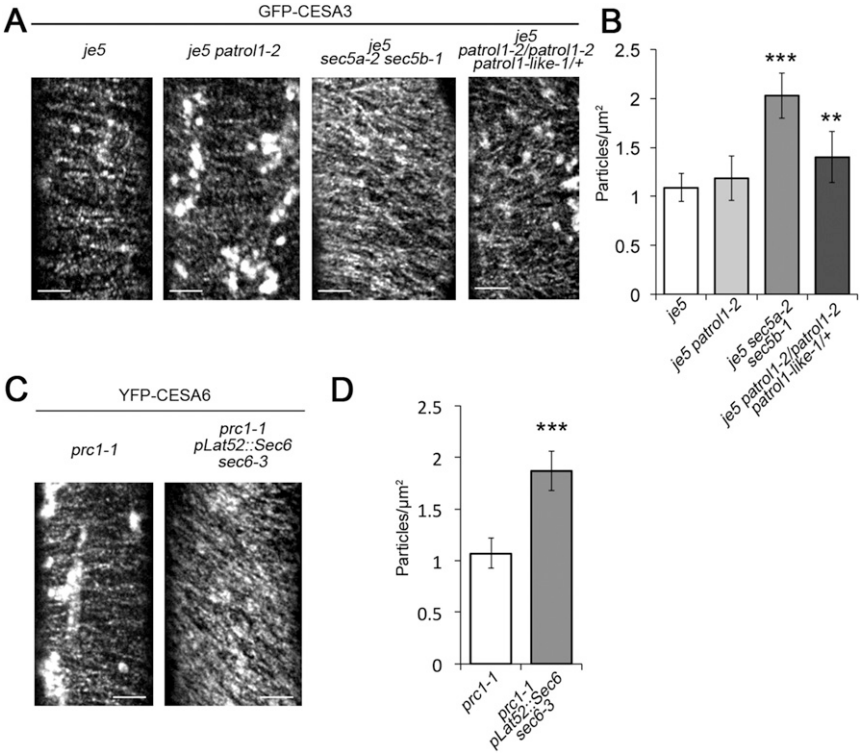

Fig. S8. The density of CSC on the PM is increased in the *PATROL1/PATROL1-LIKE* mutants and exocyst mutants. (*A*) Single-frame images displaying GFP–CESA3 particle density in control (GFP–CESA3 in *je5*), *patrol1-2* (GFP–CESA3 in *je5 patrol1-2*), *patrol1-2/patrol1-2 patrol1-like-1/+* (GFP–CESA3 in *je5 patrol1-2/patrol1-2 patrol1-like-1/+*), and the *sec5a-2 sec5b-1* mutants (GFP–CESA3 in *je5 sec5a-2 sec5b-1*). (Scale bars, 5 μm.) (*B*) Quantification shows that CSC density in *patrol1-2* mutant is comparable to that in control line, but increased in *patrol1-2/patrol1-2 patrol1-like-1/+* and *sec5a-2 sec5b-1* mutants. $n = 17$ ROIs from nine cells for control; $n = 23$ ROIs from 16 cells for patrol1-2; $n = 17$ ROIs from nine cells for *sec5a-2 sec5b-1*. Error bars represent SD. $^{**}P < 0.001$, $^{***}P < 0.0001$. (*C*) Single-frame images showing YFP–CESA6 particle density in control (YFP–CESA6 in *prc1-1*) and in the *pLat52::Sec6 sec6-3* mutants (YFP–CESA6 in *je5 pLat52::Sec6 sec6-3*). (Scale bars, 5 μm.) (*D*) Quantification shows that CSC density is increased in the *pLat52::Sec6 sec6-3* mutants. $n = 17$ ROIs from 10 cells for control, $n = 20$ ROIs from 13 cells for *pLat52::Sec6 sec6-3* mutants. Error bars represent SD. $^{***}P < 0.0001$.

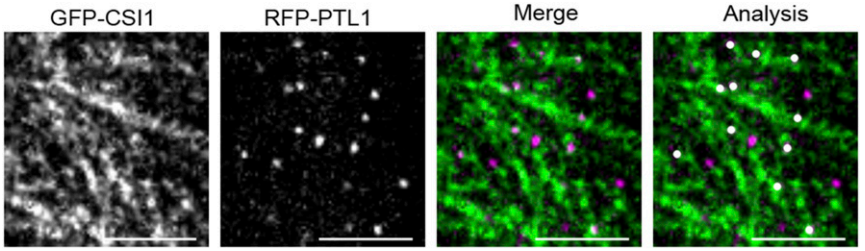

Fig. S9. PTL1 colocalizes with CSI1. Single-frame images were obtained from the GFP–CSI1 and RFP–PTL1 fluorescence signals simultaneously, and merged into one frame to visualize colocalized particles. In a representative analysis panel, white dots represent colocalized RFP–PTL1 and GFP–CSI1. (Scale bars, 5 μm.)

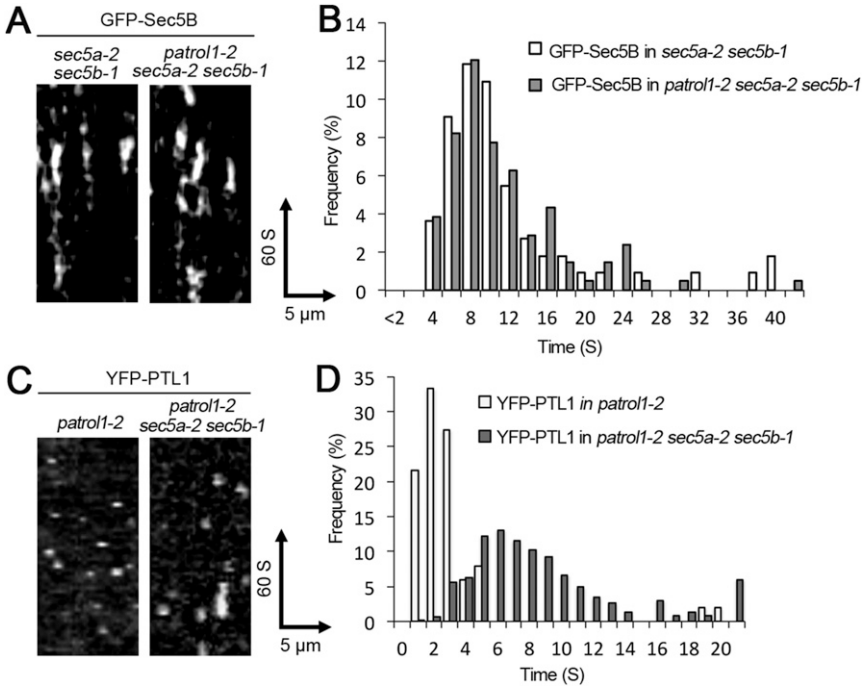

Fig. S10. PTL1 and subunits of exocyst are functionally associated. (*A* and *B*) Lesion in *PTL1* does not affect lifetimes of the exocyst complex. Kymographs were derived from a 60-s movie with 1-s interval for GFP–Sec5B in the control (GFP–Sec5B *sec5a-2 sec5b-1*) and in *patrol1-2* (GFP–Sec5B *patrol1-2 sec5a-2 sec5b-1*) mutants (*A*). The lifetime of the GFP–Sec5B particles is displayed in a histogram (*B*). $n = 110$ particles from four cells for control; $n = 207$ particles from six cells for *patrol1-2*. (*C* and *D*) The lifetimes of the PTL1 particles is prolonged in the exocyst mutant. Kymographs were derived from a 60-s movie with 1-s interval for YFP–PTL1 in the control (YFP–PTL1 in *patrol1-2*) and in the exocyst (YFP–PTL1 *patrol1-2 sec5a-2 sec5b-1*) mutant (*C*). The lifetime distribution of the YFP–PTL1 particles is displayed in a histogram (*D*). $n = 198$ from five cells for control; $n = 466$ from 27 cells for the exocyst mutant.

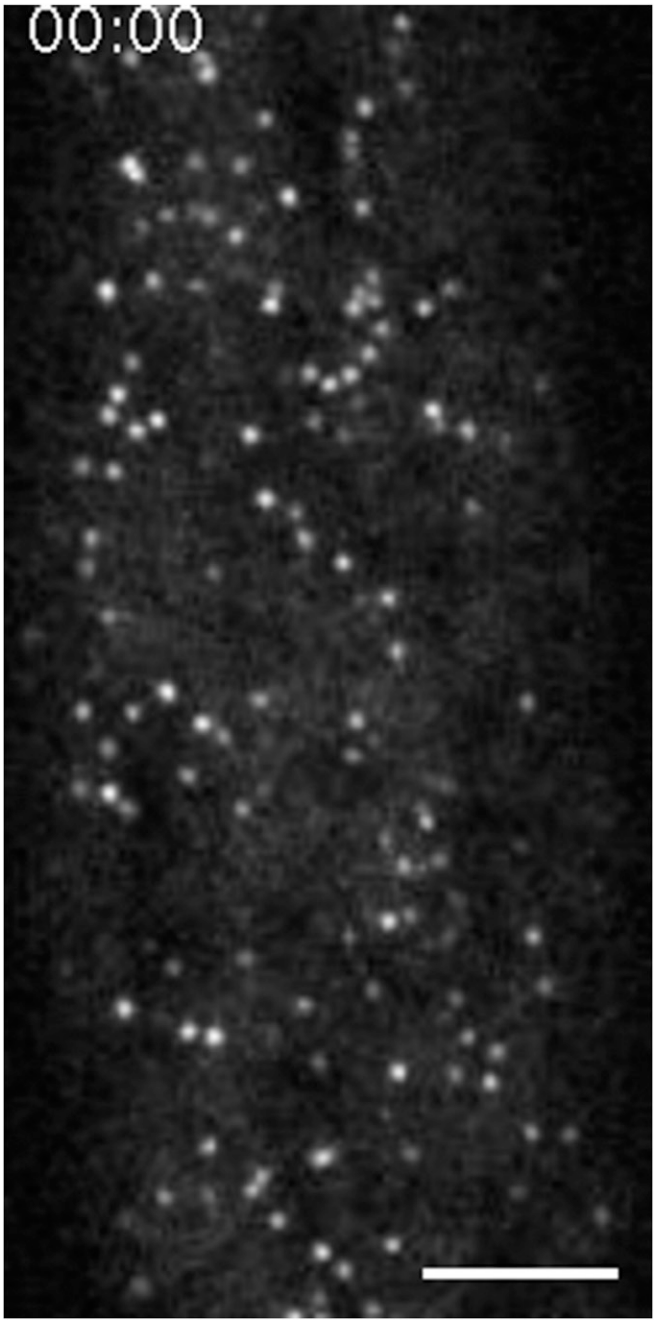

Movie S1. Dynamics of the PTL1 particles at the PM of the *Arabidopsis* etiolated hypocotyl cells. The 2.5-d-old etiolated *Arabidopsis* seedlings expressing RFP–PTL1 in *patrol1-2* were imaged by confocal microscopy. Time series are 1-s intervals. Total time = 60 s. Frame rate = 7 fps. (Scale bar, 5 μm.)

Movie S1

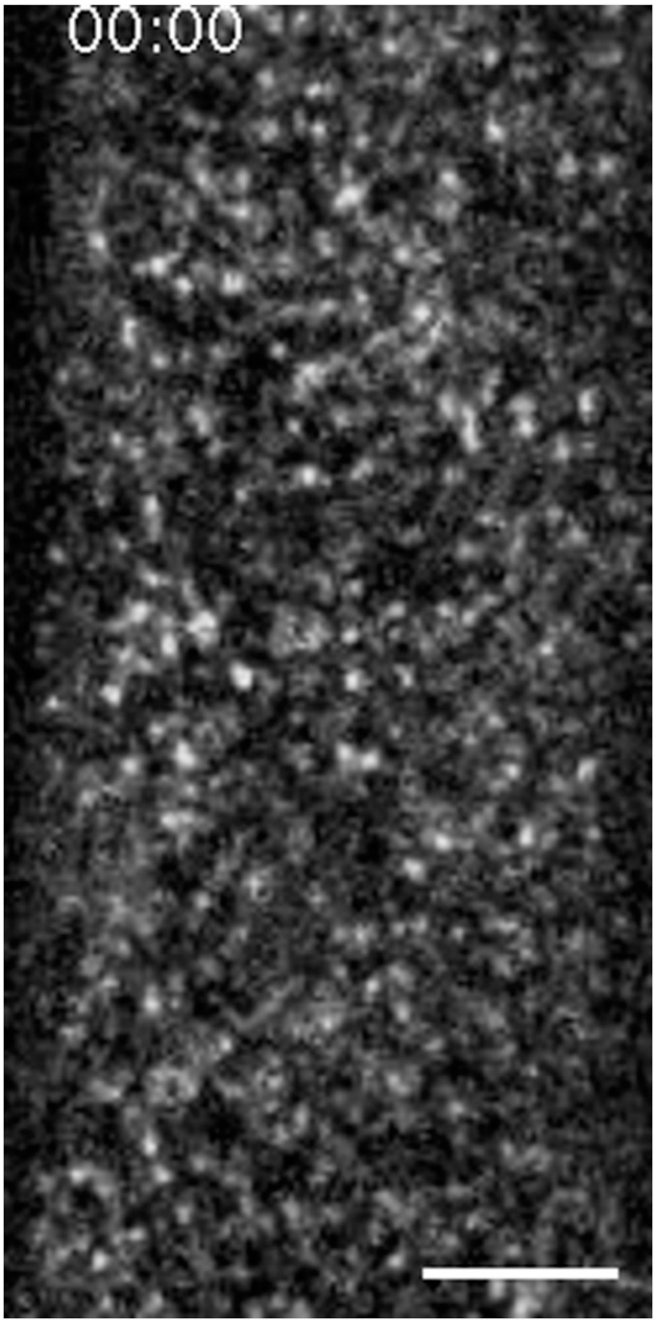

Movie S2. Dynamics of the Sec5B particles at the PM of the *Arabidopsis* etiolated hypocotyl cells. The 2.5-d-old etiolated *Arabidopsis* seedlings expressing GFP–Sec5B in *sec5a-2 sec5b-1* were imaged by confocal microscopy. Time series are 1-s intervals. Total time = 120 s. Frame rate = 7 fps. (Scale bar, 5 μm.)

Movie S2

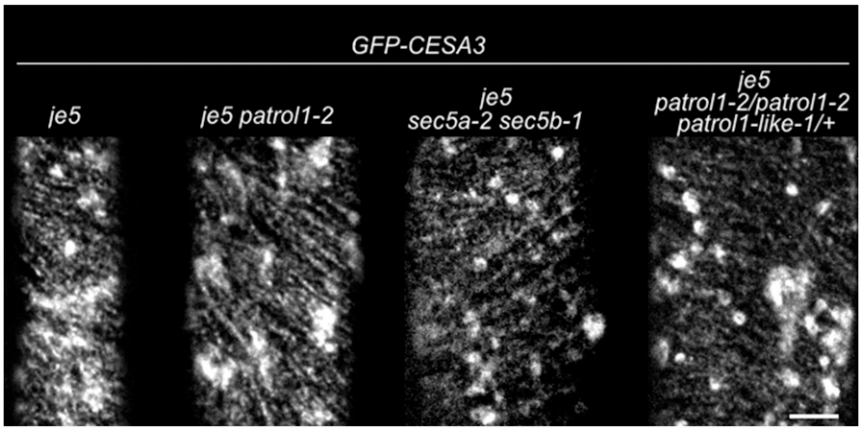

Movie S3. The motility of PM CSCs was significantly reduced in both *sec5a-2 sec5b-1* and *patrol1-2/patrol1-2 patrol1-like-1*/+ mutants. The 2.5-d-old etiolated *Arabidopsis* seedlings expressing GFP–CESA3 in *je5*, *je5 patrol1-2*, *je5 sec5a-2 sec5b-1*, and *je5 patrol1-2/patrol1-2 patrol1-like-1*/+ were imaged by confocal microscopy, respectively. Time series are 5-s intervals. Total time = 5 min. Frame rate = 7 fps. (Scale bar, 5 μm.)

Movie S3

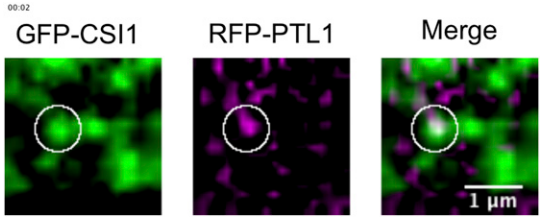

Movie S4. PTL1 colocalizes with CSI1 at the PM. The 2.5-d-old etiolated *Arabidopsis* seedlings coexpressing GFP–CSI1 and RFP–PTL1 were imaged by confocal microscopy. Circles mark the colocalized particles. Time series are 1-s intervals. Total time = 10 s. Frame rate = 7 fps. (Scale bar, 1 μm.)

Movie S4

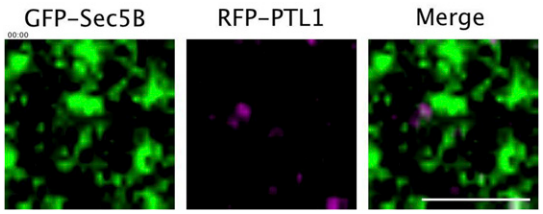

Movie S5. PTL1 colocalizes with the exocyst at the PM. The 2.5-d-old etiolated *Arabidopsis* seedlings coexpressing GFP–Sec5B and RFP–PTL1 were imaged by confocal microscopy. Circles mark the colocalized particles. Time series are 1-s intervals. Total time = 59 s. Frame rate = 7 fps. (Scale bar, 5 μm.)

Movie S5

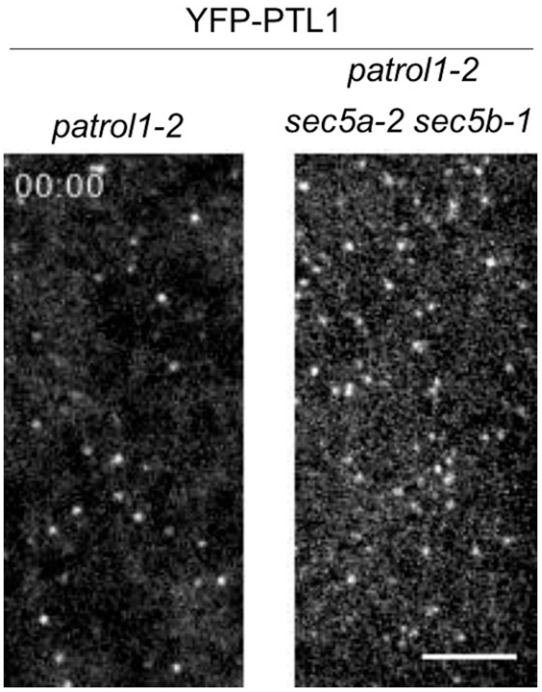

Movie S6. The lifetime of PTL1 is affected in the exocyst mutants. The 2.5-d-old etiolated *Arabidopsis* seedlings were imaged by confocal microscopy. YFP–PTL1 signal was monitored in the *patrol1-2* and *patrol1-2 sec5a-2 sec5b-1* mutant background, respectively. Time series are 1-s intervals. Total time = 59 s. Frame rate = 7 fps. (Scale bar, 5 μm.)

Movie S6

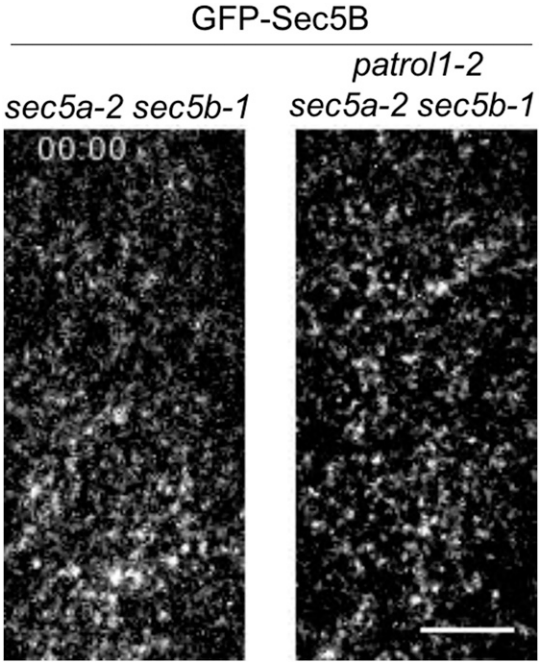

Movie S7. Lesion in *PTL1* does not affect lifetime of the exocyst complex. The 2.5-d-old etiolated *Arabidopsis* seedlings were imaged by confocal microscopy. GFP–Sec5B signal was monitored in the *sec5a-2 sec5b-1* and the *patrol1-2 sec5a-2 sec5b-1* mutant background, respectively. Time series are 1-s intervals. Total time = 146 s. Frame rate = 7 fps. (Scale bar, 5 μm.)

Movie S7

Dataset S1. Result of the yeast two-hybrid screen using the central domain of CESA6 as bait

Dataset S1

Dataset S2. List of proteins identified by ultrasensitive mass spectrometry in each of the co-IP assays

Dataset S2

Dataset S3. Segregation of *patrol1-like-1* heterozygous copy and reciprocal crossing of *patrol1-like-1* heterozygous with the Col-0 plants

Dataset S3

Dataset S4. Post hoc analysis for Fig. 4

Dataset S4

Dataset S5. List of all of the primers used in this study

Dataset S5